

BiVO₄-Based Systems Magnetron Sputtered with Silver Nanoparticles for the Artificial Photosynthesis Reaction

Eva Naughton ¹, Emerson C. Kohlrausch ², Jesum Alves Fernandes ² and James A. Sullivan ^{1,*}

¹ School of Chemistry, University College Dublin, Belfield, Dublin 4, D18 V1W8, Ireland; eva.naughton@ucd.ie

² School of Chemistry, University of Nottingham, University Park NG7 2RD, Nottingham, UK; emerson.kohlrausch@nottingham.ac.uk (E.C.K.); jesum.alvesfernandes@nottingham.ac.uk (J.A.F.)

* Correspondence: james.sullivan@ucd.ie

Catalyst Characterisation

Inductively Coupled Plasma-Optical Emission Spectroscopy (ICP-OES) was used to determine the loading of silver nanoparticles on the surface of some semiconductor materials following magnetron sputtering. The instrument used was a Perkin Elmer Optima 2000 DV equipped with an S10 Autosampler. Prior to analysis, calibration standards were prepared containing Ag concentrations of 1, 5, 10, 25, 50, and 100 ppm, and a calibration curve of relevant emission intensity vs. concentration was generated. The samples were digested in concentrated nitric acid at room temperature overnight to ensure complete dissolution.

Solid-state Ultraviolet-Visible Spectroscopy (UV-Vis) measurements were carried out on a Jasco V-650 instrument equipped with an integrating sphere (ISV-722) attachment. The instrument was set to absorbance mode, with a scanning range of 300–700 nm, data intervals of 1 nm, UV-Vis bandwidth of 2 nm, medium response, and a scan speed of 400 nm/min.

Tauc Plots were used to estimate the band gaps of the materials. The “Kubelka-Munk” equation transforms the reflectance spectra to the corresponding absorbance spectra using the following formula:

$$F(R_{\infty}) = (1 - R_{\infty})^2 / 2R_{\infty} \quad (1)$$

To generate a Tauc plot, $F(R_{\infty})$ is multiplied by the photon energy ($h\nu$) and raised to the power of $1/\gamma$, where γ is 0.5 and 2 for direct and indirect band gap semiconductors, respectively.

$$(F(R_{\infty})h\nu)^{1/\gamma} \quad (2)$$

This is then plotted against the energy of light (eV), and linear extrapolation of the curve to 0 yields the band gap of the material.

A SIEMENS D500 Kristalloflex diffractometer was used for powder X-ray Diffraction (XRD) analysis using Cu K α radiation ($\lambda = 0.154056$ nm). Voltage and current were set to 40 kV and 30 mA, respectively, and the scan was conducted in 2θ mode, with an angular range of 20–90°, 0.02 steps per degree and 2 s per step.

Transmission Electron Microscopy (TEM) images were acquired on a FEI Tecnai G2 20 Twin Microscope operating at 200 kV. Samples were dispersed in water (1 mg/mL) and sonicated for 15 min. An amount of 5 μ L of the suspension was dropped onto holey carbon films supported by TEM copper meshes and allowed to dry.

For Carbon Dioxide Temperature Programmed Desorption (CO₂-TPD) analysis, 20 mg of sample was placed inside a glass tube reactor, which was then secured in a tube furnace. Argon was flowed over the catalyst at a rate of 100 mL/min for 30 min at 110 °C. The temperature was cooled to 50 °C and CO₂ (5 mL/min) and Ar (95 mL/min) were flowed for a further 30 min. The flow was then switched back to Ar (100 mL/min). The inert flow continued until pCO₂ (as measured by an online MS) returned to background levels and the furnace was at room temperature. The furnace was then set to a target

temperature of 700 °C at a ramp rate of 10 °C/min, and an online ThermoOnix Prolab mass spectrometer was used to detect desorbed species with $m/z = 44$, *i.e.*, CO₂.

A Brunauer–Emmett–Teller (BET) analysis was conducted in order to determine the surface areas of the materials. The experiments were performed on a Quantachrome Autosorb-iQ instrument at the boiling point of Nitrogen (77.3 K). Prior to data collection, the sample surfaces were cleaned in a degas treatment (where the sample was heated to 250 °C for 10 h under secondary vacuum); then, the sample chamber was evacuated.

Infrared (IR) spectroscopy was carried out on a Bruker Alpha ATR-IR Spectrometer. A background spectrum was recorded prior to spectra collection; then, samples were analysed with light between 4000 and 500 cm⁻¹, with a resolution of 4 cm⁻¹ and a recording of 28 scans.

Results and Discussion

TEM

These show the particle sizes across all three samples. Neither Ag nor BiVO₄ were monodisperse, with both having a large distribution of particle sizes. Ag has been shown to be unstable under the electron beam used in these measurements. Li et al. have reported that, when Ag NPs were exposed to an electron beam, they became very surface active and unstable. The particles then agglomerated and, in doing so, reduced their surface energies. This converts the surface energy to thermal energy, which can then further result in their subsequent sublimation [56]. This may have led to the aggregation of Ag particles, leading to the overall measured average particle size being higher than it is in reality. The average size of BiVO₄ across the three samples determined using ImageJ analysis was 683 nm. This agrees with the literature report from which the synthesis was obtained where the BiVO₄ average particle size was in the micrometre range [32]. The average BiVO₄ particle size did not change in a major way from sample to sample, showing that the sputtering process did not noticeably damage or erode the surfaces of the particles or break them into smaller pieces.

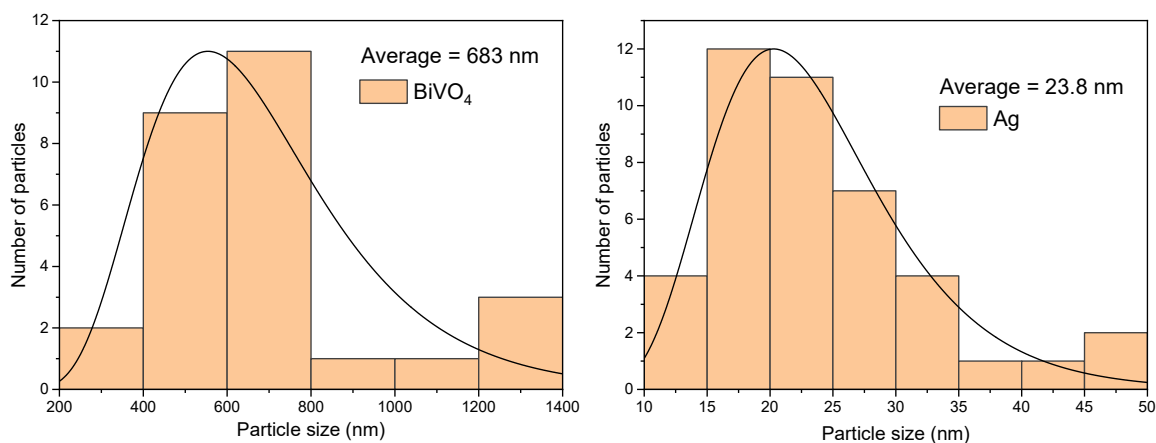


Figure S1. Particle size distribution histograms across all three samples of BiVO₄ (left), and Ag (right).

BET

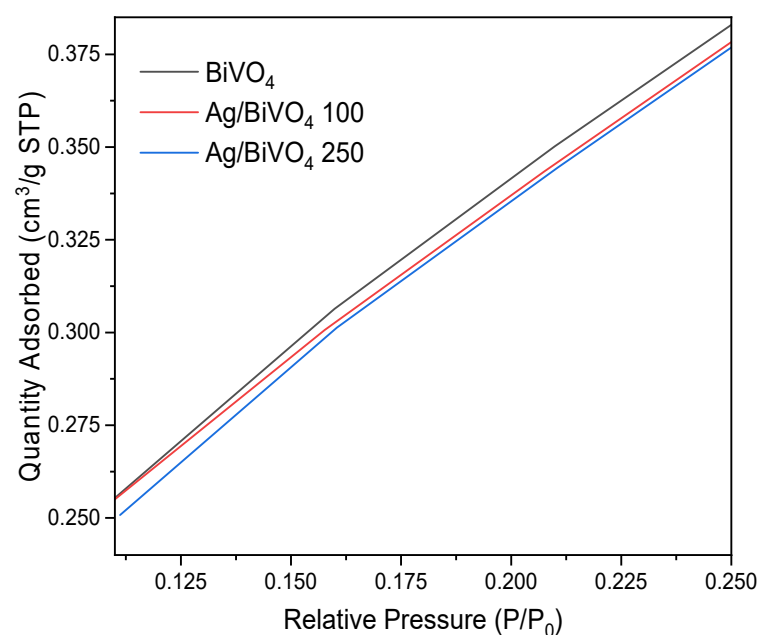


Figure S2. BET plots for BiVO₄ and the Ag-sputtered materials.

Post-reaction Characterisation

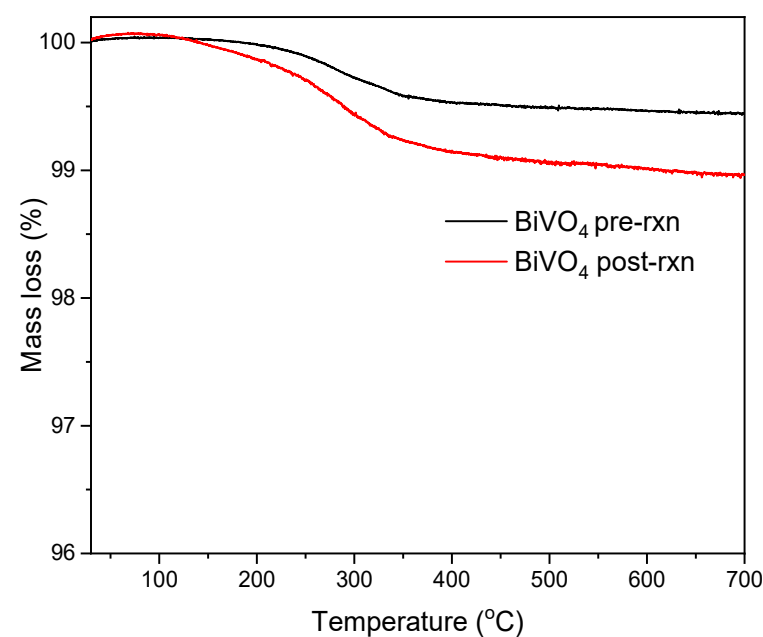


Figure S3. TGA profile of BiVO₄ pre and post AP reaction.

References

56. Li, Y.; Duan, X.; Qian, Y.; Yang, L.; Liao, H. Nanocrystalline Silver Particles: Synthesis, Agglomeration, and Sputtering Induced by Electron Beam. *J. Colloid Interface Sci.* **1999**, *209*, 347–349, doi:10.1006/jcis.1998.5879.
32. Bai, S.; Li, Q.; Han, N.; Zhang, K.; Tang, P.; Feng, Y.; Luo, R.; Li, D.; Chen, A. Synthesis of novel BiVO₄/Cu₂O heterojunctions for improving BiVO₄ towards NO₂ sensing properties. *J. Colloid Interface Sci.* **2020**, *567*, 37–44, doi:10.1016/j.jcis.2020.01.104.